TECHNICAL RESEARCH REPORT

SYSTEMS RESEARCH CENTER

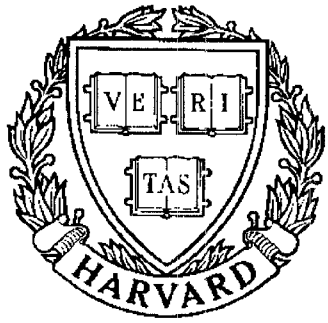

Supported by the National Science Foundation Engineering Research Center Program (NSFD CD 8803012), the University of Maryland, Harvard University, and Industry

Torque Resolver Design for Tendon-Drive Manipulators

by J.-J. Lee and L.-W. Tsai

TR 91-52

Torque Resolver Design for Tendon-Driven Manipulators

Jyh-Jone Lee
Graduate Research Assistant

Lung-Wen Tsai
Member of ASME
Professor

Mechanical Engineering Department
and
Systems Research Center
University of Maryland
College Park, MD 20742

Abstract

Given desired joint torques in an n-DOF tendon-driven manipulator with $n+1$ control tendons, the determination of tendon forces is an indeterminate problem. Usually, the pseudo-inverse technique can be used to solve for such a problem. In this paper, rather than using the pseudo-inverse technique, an efficient methodology for transforming joint torques (n elements) to motor torques ($n+1$ elements) has been developed. This technique, called "torque resolver", utilizes two circuit-like operators to transform torques between two different vector spaces. It can be easily programmed on a digital computer or implemented into an analog-circuit system. It is hoped that this technique will make real-time control using computed torque method feasible. The technique has been demonstrated through the dynamic simulation of a three-DOF manipulator.

1. Introduction

Tendons have commonly been used as power transmission elements in the design of dextrous hands, for they allow actuators to be installed remotely from the joint they drive. The application of tendons for power transmission may reduce the inertia and size of the manipulating system. A few tendon-driven mechanical systems can be found in the literature (Jacobsen, et al., 1984; Morecki, et al., 1980; Okada, 1977; Pham and Heginbotham, 1986; and Salisbury, 1982).

A special characteristic associated with tendon-driven manipulators is that tendons can only exert tension. In other words, force can only be transmitted from actuators to the joints in a unidirectional sense. This characteristic imposes certain constraints on tendon routing (Morecki, et al., 1980; and Lee and Tsai, 1991). As a result, it increases the complexity in the control of such manipulating systems, e.g. the coupling of displacements, and the redundancy in tendon forces. The purpose of this investigation is to establish a systematic methodology for the resolution of redundancy of tendon forces. The methodology will be illustrated by three different kinematic structures of tendon-driven manipulators. Using this concept, the control of a tendon-driven manipulator will be demonstrated via the dynamic simulation

of a three-DOF (Degree-Of-Freedom) tendon-driven manipulator.

First, a dynamic model and a simple control algorithm based on the computed torque method for an n-DOF tendon-driven manipulator having $(n+1)$ tendons will be reviewed. The model assumes that friction and compliance in tendons can be neglected. Then, a methodology for transforming joint torques to motor torques will be introduced. This procedure, called "torque resolver", uses two circuit-like operators to compute tendon forces in terms of joint torques. It can be easily programmed on a digital computer or implemented into an analog-circuit system.

2. Dynamic Modelling

Figure 1 shows an n-DOF manipulator with $(n+1)$ tendons. The dynamics of such a system can be formulated from two subsystems: the open-loop chain and the rotors. The dynamic equations of an open-loop chain without gravity term can be expressed as (Paul, 1981):

$$M(\theta)\,\underline{\ddot{\Theta}} + \underline{h}(\theta,\dot{\theta}) = \underline{\tau} \tag{1}$$

where $M(\theta)$ is an $n \times n$ inertia matrix, $\underline{\Theta}$ an $n \times 1$ vector representing the joint angles θ, $\underline{h}(\theta,\dot{\theta})$ an $n \times 1$ vector representing the Centrifugal and Coriolis terms, and $\underline{\tau}$ an $n \times 1$ vector representing the resultant joint torques in the open-loop chain.

The motor rotor dynamics can be approximated by a second-order system. Consider the ith motor-tendon spooling system as shown in Fig. 2. If the ith tendon is wound around the ith pulley of radius r_{m_i}, and the pulley is coupled to a gear reducer having a gear ratio of $n_i = r_g/r_p$ $(n_i \geq 1)$, then torque developed by the ith motor is equal to the sum of inertia torque, friction torque, and the torque reflected at the motor shaft due to tendon force, i.e.

$$j_{m_i}\ddot{\theta}_{m_i} + c_{m_i}\dot{\theta}_{m_i} + \frac{r_{m_i}}{n_i} f_i = \xi_i \tag{2.a}$$

where j_{m_i}, c_{m_i}, θ_{m_i}, f_i, and ξ_i denote rotor inertia, viscous-friction coefficient, rotor angular displacement, tension in the ith tendon, and torque developed by the ith motor, respectively.

Since there are $n+1$ motors for an n-DOF tendon-driven manipulator, Eq. (2.a) can be written $n+1$ times, once for each motor. These $n+1$ dynamic equations can be compiled into a matrix form as:

$$J_m\underline{\ddot{\Theta}}_m + C_m\underline{\dot{\Theta}}_m + R_m\underline{F} = \underline{\xi} \tag{2.b}$$

where J_m, C_m, and R_m are $(n+1)\times(n+1)$ diagonal matrices whose diagonal elements are j_{m_i}, c_{m_i}, and $\frac{r_{m_i}}{n_i}$, respectively; and $\underline{\Theta}_m$ and $\underline{\xi}$ are $(n+1)\times 1$ vectors whose elements are the rotor angular displacements and motor torques, respectively.

The force and displacement relationship between the joint space and tendon space have been developed by Tsai and Lee (1989). The resultant joint torques, $\underline{\tau} = (\tau_n, \tau_{n-1}, \cdots, \tau_2, \tau_1)^T$, is related to tendon forces, $\underline{F} = (f_1, f_2, \cdots, f_{n+1})^T$, by the equation

$$\underline{\tau} = R^T B^T \underline{F} \tag{3.a}$$

where it is assumed that all pulleys pivoted about one joint axis are of the same radii, and the matrix B^T whose elements consist of -1, 0, and +1 is an $n\times(n+1)$ matrix, and the matrix R^T whose non-zero elements are the radii of the pulleys is an $n\times n$ diagonal matrix.

The linear displacement of tendons, $\underline{S} = (s_1, s_2, \cdots, s_{n+1})^T$, is related to the joint angles, $\underline{\Theta} = (\theta_n, \theta_{n-1}, \cdots, \theta_2, \theta_1)^T$, by the equation

$$\underline{S} = BR\underline{\Theta} \tag{3.b}$$

Hence, rotor angular displacements can be related to the manipulator joint angles by $R_m\underline{\Theta}_m = BR\underline{\Theta}$. Eliminating $\underline{\Theta}_m$ between this equation and Eq. (2.b), one can solve tendon forces in terms of motor torques and joint angles as:

$$\underline{F} = {R_m}^{-1}[\underline{\xi} - J_m{R_m}^{-1}BR\underline{\ddot{\Theta}} - C_m{R_m}^{-1}BR\underline{\dot{\Theta}}] \tag{4}$$

Substituting Eqs. (4) and (3.a) into (1), yields

$$(M + \tilde{M})\underline{\ddot{\Theta}} + \tilde{C}_m\underline{\dot{\Theta}} + \underline{h}(\theta,\dot{\theta}) = R^T B^T {R_m}^{-1}\underline{\xi} \tag{5}$$

where $\tilde{M} = R^T B^T {R_m}^{-1} J_m {R_m}^{-1} BR$ and $\tilde{C}_m = R^T B^T {R_m}^{-1} C_m {R_m}^{-1} BR$.

Equation (5) completely describes the dynamics of a tendon-driven manipulator. The term $\tilde{M}$ gives the effect of rotor inertia to the dynamics of the system and the term $\tilde{C}_m$ gives the effect of rotor damping. It should be noted that tendon tensions given by Eq.(4) must be positive at all times for the dynamic model to be valid. In Section 5, a heuristic will be developed to guarantee positive tension in tendons.

3. Computed Torque Controller

The "computed torque" technique can be implemented for controlling the manipulator. The technique assumes that one can accurately compute the configuration dependent variables, $M(\theta)$ and $\underline{h}(\theta, \dot{\theta})$, in real time to minimize the nonlinear effect. It uses a proportional plus a derivative feedback to servo the motors.

Let the computed torque $\underline{\tau}_{cm}$ be related to the motor torques by

$$\underline{\tau}_{cm} = R^T B^T {R_m}^{-1} \underline{\xi} \tag{6.a}$$

and let the value of $\underline{\tau}_{cm}$ be computed from joint feedback signals as

$$\underline{\tau}_{cm} = (M + \tilde{M})[\underline{\ddot{\Theta}}_d + K_v \underline{\dot{e}} + K_p \underline{e}] + \tilde{C}_m \underline{\dot{\Theta}} + \underline{h}(\theta, \dot{\theta}) \tag{6.b}$$

where K_v and K_p are respectively $n \times n$ derivative and position feedback gain matrices, $\underline{\Theta}_d$ is the desired joint angular displacement vector, and $\underline{e} \equiv \underline{\Theta}_d - \underline{\Theta}$ is the error vector. Substituting Eqs.(6.a) and (6.b) into (5) and after some simplification, yields

$$(M + \tilde{M})(\underline{\ddot{e}} + K_v \underline{\dot{e}} + K_p \underline{e}) = 0 \tag{7}$$

Since $(M + \tilde{M})$ is positive definite, one can choose K_v and K_p appropriately so that the characteristic roots of Eq. (7) have proper negative real parts and the tracking error $\underline{e}(t)$ approaches zero asymptotically.

Note that since the vector spaces of $\underline{\tau}_{cm}$ and $\underline{\xi}$ do not have the same dimensions, the mapping from the joint torque space to the actuator torque space is not unique.

Given $\underline{\tau}_{cm}$, the solution of $\underline{\xi}$ can be obtained by the pseudo-inverse of Eq. (6.a). The result can be expressed as the summation of a particular solution and a homogeneous solution as:

$$\underline{\xi} = (R^T B^T {R_m}^{-1})^+ \ \underline{\tau}_{cm} + \lambda \underline{\xi}_h \tag{8}$$

where $(\#)^+ = \{(\#)^T[(\#)(\#)^T]^{-1}\}$ represents the pseudo-inverse of $(\#)$ (Strang 1980), $\underline{\xi}_h$ lies in the null space of matrix $(R^T B^T {R_m}^{-1})$, and λ is an arbitrary constant. The components of $\underline{\xi}_h$ must be of the same sign, thus, by adjusting λ, motor torques can be increased unidirectionally to assure positive tension in all tendons.

The pseudo-inverse method is very inefficient in computation. In what follows, we will develop a more efficient method to resolve the motor torques.

4. Torque Resolver

As mentioned in the previous section, given desired joint torques, the determination of tendon forces (or motor torques) is an indeterminate problem. For an $n \times (n+1)$ system, the pseudo-inverse technique can be used to solve for tendon forces. The computation of the pseudo-inverse method is very time consuming. In addition, the constant λ in Eq. (8) must be chosen properly such that all the tendons are under tension. To achieve this, the largest ratio of all the negative tendon forces in the particular solution to their corresponding components in the homogeneous solution must be identified. This process will inevitably increase the computation time and reduce the possibility for real time control of the system.

Another method proposed by Jacobsen et al. (1984, 1989) is to use the "rectifier" concept to determine appropriate tendon tensions. This method, without going through the pseudo-inverse formulation, uses circuit-like operators to convert joint torque signals to tendon tension signals. It provides a closed-form-like solution to determine the necessary tendon tensions and can be implemented by analog circuits. Nonetheless, the result developed by Jacobsen, et al. is solely applicable to the Utah/MIT hand in which the tendon forces are less coupled than that of

the $n \times (n+1)$ systems. In what follows, this concept will be generalized for the $n \times (n+1)$ systems. It will be shown that this concept can be systematized.

Basic Principle

A one-DOF system is used to illustrate the basic principle. Figure 3 shows the schematic of a one-DOF manipulator controlled by two tendons. Defining the positive direction of rotation for the joint to be pointing out of the paper and τ_0 the resultant joint torque to be generated, then the force equation for the system can be written as:

$$f_2 - f_1 = \tau_0 / r_0 \tag{9}$$

where r_0 is the pulley radius.

Equation (9) contains only two unknown variables, f_1 and f_2, both of which must be positive at all times. If τ_0 is positive (counterclockwise), the minimum forces required will be τ_0/r_0 for f_2 and zero for f_1. On the other hand, if τ_0 is negative (clockwise), the minimum forces will be $-\tau_0/r_0$ for f_1 and zero for f_2. This simple relation can be written in a mathematical form as shown below:

$$\begin{cases} f_1 = \delta_0 \\ f_2 = \tau_0/r_0 + \delta_0, \end{cases} \qquad if\ \tau_0 \geq 0 \tag{10.a}$$

and

$$\begin{cases} f_1 = -\tau_0/r_0 + \delta_0 \\ f_2 = \delta_0, \end{cases} \qquad if\ \tau_0 < 0 \tag{10.b}$$

where δ_0 is a positive biased force which has no net effect on the resultant joint torque τ_0.

Define the operators O^+ and O^- as

$$O^+(x) = \begin{cases} x, & x \geq 0; \\ 0, & x < 0 \end{cases} \tag{11.a}$$

and

$$O^-(x) = \begin{cases} 0, & x \geq 0; \\ -x, & x < 0 \end{cases} \tag{11.b}$$

where x is a dummy variable. The characteristics of $O^+(x)$ and $O^-(x)$ can be described graphically as shown in Fig. (4). Mathematically, $O^+(x)$ and $O^-(x)$ can also be written as

$$O^+(x) = [x + |x|]/2 \tag{11.c}$$

and

$$O^-(x) = [-x + |x|]/2 \tag{11.d}$$

Note that $O^+(x) + O^-(x) = |x|$, and $O^+(x) - O^-(x) = x$.

Expressing Eqs. (10.a) and (10.b) in terms of O^+ and O^- operators, yields

$$\begin{cases} f_1 = O^-(\tau_0/r_0) + \delta_0 \\ f_2 = O^+(\tau_0/r_0) + \delta_0 \end{cases} \tag{12}$$

We note that the O^+ operator goes with the variable with a positive sign and the O^- operator goes with the variable with a negative sign in Eq. (9). The physical meaning of Eq. (12) can be readily seen from Fig. 3. If the joint torque required is positive, then tendon f_2 must have a minimum pull of magnitude τ_0/r_0 while f_1 remains zero. On the other hand, if the joint torque required is negative, then tendon f_1 must have a pull of magnitude $|\tau_0/r_0|$ while f_2 remains zero. Adding a biased force δ_0 to both f_1 and f_2 has no influence on the equilibrium of τ_0. The ratio of the biased forces in two tendons, 1:1 for this simple system, is proportional to the homogeneous solution to Eq. (9).

5. Application to Multi-DOF Systems

The application of $O^+(x)$ and $O^-(x)$ operators to a general n-DOF system leads to a systematic approach for the determination of tendon forces without using the pseudo-inverse technique. In general, the system of equations shown in Eq. (3.a) will be reduced to such an extent that one of the equations contains only two unknown variables. Then, the solution for the two unknown forces can be obtained by applying the $O^+(x)$ and $O^-(x)$ operators. This process can be repeated until

all the variables are solved. The following three examples are designed to illustrate the methodology.

Example 1. Structure Matrix in Pseudo-Triangular Form

Consider the planar representation (Tsai and Lee, 1989) of a spatial three-DOF manipulator shown in Fig. 5(a). The structure matrix B^T has a pseudo-triangular form (Lee and Tsai, 1991):

$$B^T = \begin{bmatrix} -1 & 1 & 0 & 0 \\ -1 & -1 & 1 & 0 \\ -1 & -1 & -1 & 1 \end{bmatrix}.$$

The homogeneous solution is given by $[1\ 1\ 2\ 4]^T$. Substituting the structure matrix into Eq. (3.a) and inverting the radius matrix R^T to the left-hand-side of the equation, yields

$$-f_1 + f_2 = \tau_3/r_3 \tag{13.a}$$

$$-f_1 - f_2 + f_3 = \tau_2/r_2 \tag{13.b}$$

$$-f_1 - f_2 - f_3 + f_4 = \tau_1/r_1 \tag{13.c}$$

Since Eq. (13.a) contains only two unknowns, f_1 and f_2, and they must be positive at all times, we can write f_1 and f_2 in terms of O^+ and O^- operators as

$$\begin{cases} f_1 = O^-(\tau_3/r_3) + \delta_1 \\ f_2 = O^+(\tau_3/r_3) + \delta_1 \end{cases} \tag{14}$$

To determine f_3, we substitute Eq. (14) into Eq. (13.b) and apply the relation $O^-(x) + O^+(x) = |x|$. This yields

$$-2\delta_1 + f_3 = \tau_2/r_2 + |\tau_3/r_3| \tag{15}$$

Note that Eq. (15) contains two unknowns, δ_1 and f_3. Following the same reasoning, one can conclude that if the value of $(\tau_2/r_2 + |\tau_3/r_3|)$ is positive, then the minimum force will be $(\tau_2/r_2 + |\tau_3/r_3|)$ for f_3 and zero for δ_1. On the other hand, if $(\tau_2/r_2 +$

$|\tau_3/r_3|$) is negative, then the minimum forces will be zero for f_3 and $(-\tau_2/r_2 - |\tau_3/r_3|)$ for $2\delta_1$. This can be mathematically expressed as:
For $(\tau_2/r_2 + |\tau_3/r_3|) \geq 0$, then

$$\begin{cases} 2\delta_1 = \delta_2 \\ f_3 = \tau_2/r_2 + |\tau_3/r_3| + \delta_2, \end{cases} \tag{16.a}$$

else

$$\begin{cases} 2\delta_1 = -\tau_2/r_2 - |\tau_3/r_3| + \delta_2 \\ f_3 = \delta_2 \end{cases} \tag{16.b}$$

where δ_2 is a positive biased force which will result in no net joint torque about joint 2. Writing Eqs.(16.a) and (16.b) in terms of the O^+ and O^- operators, yields

$$\begin{cases} \delta_1 = O^-(\tau_2/r_2 + |\tau_3/r_3|)/2 + \delta_2/2 \\ f_3 = O^+(\tau_2/r_2 + |\tau_3/r_3|) + \delta_2 \end{cases} \tag{17}$$

Combining Eqs. (14) and (17), yields

$$f_1 = O^-(\tau_3/r_3) + O^-(\tau_2/r_2 + |\tau_3/r_3|)/2 + \delta_2/2 \tag{18.a}$$

$$f_2 = O^+(\tau_3/r_3) + O^-(\tau_2/r_2 + |\tau_3/r_3|)/2 + \delta_2/2 \tag{18.b}$$

$$f_3 = O^+(\tau_2/r_2 + |\tau_3/r_3|) + \delta_2 \tag{18.c}$$

The physical meaning of Eqs. (16.a) and (16.b) can also be explained from the tendon routing shown in Fig. 5(b). Both f_1 and f_2 pull to the right while f_3 pulls to the left of the pulleys at joint 2. The two tendons f_1 and f_2 always produce a net force of $|\tau_3/r_3|$ in addition to that from the biased force. Hence, to generate a desired torque of τ_2 at joint 2, the force difference between f_3 and that from the biased force $2\delta_1$ must be equal to $(\tau_2/r_2 + |\tau_3/r_3|)$. If it is positive, then the minimum forces will be $(\tau_2/r_2 + |\tau_3/r_3|)$ for f_3 and zero for δ_1. If it is negative, then the minimum forces will be zero for f_3 and one-half of $(\tau_2/r_2 + |\tau_3/r_3|)$ for δ_1. The biased force δ_2 is added to adjust torque about the first joint axis. Note that adding $\delta_2/2$, $\delta_2/2$, and δ_2 to f_1, f_2, and f_3, respectively has no effect on the net joint torques τ_3 and τ_2.

Likewise, substituting Eqs. (18.a,b,c) into Eq. (13.c), yields

$$-2\delta_2 + f_4 = \tau_1/r_1 + \left|\tau_2/r_2 + |\tau_3/r_3|\right| + |\tau_3/r_3| \tag{19.a}$$

Following the same reasoning, one concludes that

$$\begin{cases} \delta_2 = O^-(\tau_1/r_1 + \left|\tau_2/r_2 + |\tau_3/r_3|\right| + |\tau_3/r_3|)/2 + \delta_3/2 \\ f_4 = O^+(\tau_1/r_1 + \left|\tau_2/r_2 + |\tau_3/r_3|\right| + |\tau_3/r_3|) + \delta_3 \end{cases} \tag{19.b}$$

where δ_3 is a positive biased force.

Combining Eqs. (19.b) and (18), yields

$$\begin{cases} f_1 = O^-(\tau_3/r_3) + O^-(\tau_2/r_2 + |\tau_3/r_3|)/2 \\ \quad +O^-(\tau_1/r_1 + \left|\tau_2/r_2 + |\tau_3/r_3|\right| + |\tau_3/r_3|)/4 + \delta_3/4 \\ f_2 = O^+(\tau_3/r_3) + O^-(\tau_2/r_2 + |\tau_3/r_3|)/2 \\ \quad +O^-(\tau_1/r_1 + \left|\tau_2/r_2 + |\tau_3/r_3|\right| + |\tau_3/r_3|)/4 + \delta_3/4 \\ f_3 = O^+(\tau_2/r_2 + |\tau_3/r_3|) + O^-(\tau_1/r_1 + \left|\tau_2/r_2 + |\tau_3/r_3|\right| + |\tau_3/r_3|)/2 + \delta_3/2 \\ f_4 = O^+(\tau_1/r_1 + \left|\tau_2/r_2 + |\tau_3/r_3|\right| + |\tau_3/r_3|) + \delta_3 \end{cases} \tag{20}$$

Equation (20) provides an alternative method for the transformation of joint torques to tendon forces other than the pseudo-inverse formulation. The result guarantees that each tendon force is greater than or equal to zero. It can be seen that the computation is more straight forward than that of the pseudo-inverse technique. It should be noticed that the biased force δ_3 can be chosen arbitrarily beforehand and its effect on the joint torques is in accordance with that of the homogeneous solution.

Example 2. The Stanford/JPL Finger

The planar representation of the kinematic structure of the Stanford/JPL finger is shown in Fig. 6. The corresponding structure matrix is given by

$$B^T = \begin{bmatrix} -1 & 1 & 0 & 0 \\ -1 & 1 & -1 & 1 \\ -1 & -1 & 1 & 1 \end{bmatrix}.$$

The homogeneous solution is given by $[1\ 1\ 1\ 1]^T$. Substituting B^T into Eq. (3.a), yields the force equations

$$-f_1 + f_2 = \tau_3/r_3 \tag{21.a}$$

$$-f_1 + f_2 - f_3 + f_4 = \tau_2/r_2 \tag{21.b}$$

$$-f_1 - f_2 + f_3 + f_4 = \tau_1/r_1 \tag{21.c}$$

Since Eq. (21.a) contains only two unknowns, f_1 and f_2 can be written in terms of O^+ and O^- as,

$$\begin{cases} f_1 = O^-(\tau_3/r_3) + \delta_1 \\ f_2 = O^+(\tau_3/r_3) + \delta_1 \end{cases} \tag{22}$$

where δ_1 is a positive biased force which has no influence on joint torques τ_2 and τ_3.

Substituting Eq. (22) into (21.b), yields

$$-f_3 + f_4 = \tau_2/r_2 - \tau_3/r_3 \tag{23}$$

Hence, f_3 and f_4 can be written as

$$\begin{cases} f_3 = O^-(\tau_2/r_2 - \tau_3/r_3) + \delta_2 \\ f_4 = O^+(\tau_2/r_2 - \tau_3/r_3) + \delta_2 \end{cases} \tag{24}$$

where δ_2 is a positive biased force which has no influence on torque τ_2.

Substituting Eqs. (22) and (24) into (21.c), yields

$$-2\delta_1 + 2\delta_2 = \tau_1/r_1 + |\tau_3/r_3| - |\tau_2/r_2 - \tau_3/r_3| \tag{25}$$

Hence, δ_1 and δ_2 can be written in terms of the O^+ and O^- operators as

$$\begin{cases} \delta_1 = O^-(\tau_1/r_1 + |\tau_3/r_3| - |\tau_2/r_2 - \tau_3/r_3|)/2 + \delta_3 \\ \delta_2 = O^+(\tau_1/r_1 + |\tau_3/r_3| - |\tau_2/r_2 - \tau_3/r_3|)/2 + \delta_3 \end{cases} \tag{26}$$

where δ_3 is a positive biased force which has no effect on joint torques τ_1, τ_2, and τ_3.

Substituting Eq. (26) into (22) and (24), yields

$$\begin{cases} f_1 = O^-(\tau_3/r_3) + O^-(\tau_1/r_1 + |\tau_3/r_3| - |\tau_2/r_2 - \tau_3/r_3|)/2 + \delta_3 \\ f_2 = O^+(\tau_3/r_3) + O^-(\tau_1/r_1 + |\tau_3/r_3| - |\tau_2/r_2 - \tau_3/r_3|)/2 + \delta_3 \\ f_3 = O^-(\tau_2/r_2 - \tau_3/r_3) + O^+(\tau_1/r_1 + |\tau_3/r_3| - |\tau_2/r_2 - \tau_3/r_3|)/2 + \delta_3 \\ f_4 = O^+(\tau_2/r_2 - \tau_3/r_3) + O^+(\tau_1/r_1 + |\tau_3/r_3| - |\tau_2/r_2 - \tau_3/r_3|)/2 + \delta_3 \end{cases} \tag{27}$$

Note that the value δ_3 can be used as a pretensioning force for the tendons.

Example 3. Fully Coupled Kinematic Structure

The kinematic structure shown in Fig. 7 is a fully coupled kinematic structure. The structure matrix is given by

$$B^T = \begin{bmatrix} -1 & -1 & 1 & 1 \\ 1 & -1 & -1 & 1 \\ -1 & 1 & -1 & 1 \end{bmatrix}$$

The homogeneous solution is given by $[1\ 1\ 1\ 1]^T$.

Substituting the structure matrix into Eq. (3.a), yields

$$-f_1 - f_2 + f_3 + f_4 = \tau_3/r_3 \tag{28.a}$$

$$f_1 - f_2 - f_3 + f_4 = \tau_2/r_2 \tag{28.b}$$

$$-f_1 + f_2 - f_3 + f_4 = \tau_1/r_1 \tag{28.c}$$

In this case, none of the f_1, f_2, f_3, and f_4 can be determined by using just one of the above equations. Thus, some algebraic manipulations are necessary. Adding Eq. (28.a) to (28.b), yields

$$f_4 - f_2 = (\tau_3/r_3 + \tau_2/r_2)/2 \tag{29}$$

Therefore, f_2 and f_4 can be written in terms of the O^+ and O^- operators, i.e.

$$\begin{cases} f_2 = O^-(\tau_3/r_3 + \tau_2/r_2)/2 + \delta_1 \\ f_4 = O^+(\tau_3/r_3 + \tau_2/r_2)/2 + \delta_1 \end{cases} \tag{30}$$

where δ_1 is a positive biased force which produces no net torques about joints 2 and 3.

Subtracting Eq. (28.a) from (28.b), yields

$$f_1 - f_3 = (\tau_2/r_2 - \tau_3/r_3)/2 \tag{31}$$

Therefore, f_1 and f_3 can be obtained in terms of the O^+ and O^- operators as,

$$\begin{cases} f_1 = O^+(\tau_2/r_2 - \tau_3/r_3)/2 + \delta_2 \\ f_3 = O^-(\tau_2/r_2 - \tau_3/r_3)/2 + \delta_2 \end{cases} \tag{32}$$

where δ_2 is a positive biased force which produces no net torque about joints 2 and 3.

Substituting Eqs. (30) and (32) into (28.c), yields

$$\begin{aligned} 2\delta_1 - 2\delta_2 &= \tau_1/r_1 + |\tau_2/r_2 - \tau_3/r_3|/2 - |\tau_3/r_3 + \tau_2/r_2|/2 \\ &= b \end{aligned} \tag{33}$$

Hence, $\delta_1 = O^+(b)/2 + \delta_3$ and $\delta_2 = O^-(b)/2 + \delta_3$, where δ_3 is a biased force which has no effect on joint torques τ_1, τ_2, and τ_3. Substituting δ_1 and δ_2 into Eqs. (30) and (32), yields

$$\begin{cases} f_1 = O^+(\tau_2/r_2 - \tau_3/r_3)/2 + O^-(b)/2 + \delta_3 \\ f_2 = O^-(\tau_3/r_3 + \tau_2/r_2)/2 + O^+(b)/2 + \delta_3 \\ f_3 = O^-(\tau_2/r_2 - \tau_3/r_3)/2 + O^-(b)/2 + \delta_3 \\ f_4 = O^+(\tau_3/r_3 + \tau_2/r_2)/2 + O^+(b)/2 + \delta_3 \end{cases} \tag{34}$$

It can be seen that the above procedure is general and can be applied to any kind of $n \times (n+1)$ systems.

6. Implementation of the Torque Resolver

In this section, the design of the controller for a three-DOF tendon-driven manipulator using the above control algorithm is presented. The kinematic structure shown in Fig. 7 is used for illustration. Figure 8 shows the control block diagram for the system.

The controller is designed according to Eq. (7). Figure 9(a) shows the detailed diagram of the controller shown in Fig. 8, where k_{p_i}, k_{v_i}, and m_{ij} are the elements of matrices K_p, K_v, and $(M + \tilde{M})$, respectively.

As mentioned in Section 2, it is necessary to keep tendon forces positive at all times in order for the dynamic modelling to be valid. The following heuristic has been implemented to ensure positive tendon forces. In view of Eq. (4), to compensate for the uncertainty due to rotor inertia and viscous friction torques, the computed joint torques, Eq. (6.b), are first rectified through a "torque resolver", then the maximum desirable joint acceleration and velocity, $\underline{\ddot{\Theta}}_{max}$ and $\underline{\dot{\Theta}}_{max}$, are used to estimate additional motor torques, $J_m(\ddot{\theta}_m)_{max}$ and $C_m(\dot{\theta}_m)_{max}$, needed for pretensioning the tendons. These added values can be thought as the biased force δ_3 shown in Eq. (34). Figure 9(b) shows the detailed design of the resolver in accordance with Eq. (34). It can be seen that the transformation from joint signals to motor signals has been replaced by a circuit-like procedure which can be easily programmed on a digital computer or implemented into an analog circuit.

A computer program has been developed for the simulation of the response of motor torques and tendon forces using the above-mentioned heuristic. Figure 10 shows the schematic of the three-DOF manipulator used for simulation. Applying simultaneous step inputs to the three joint angles, Figs. 11 and 12 respectively depicts the response of motor torques and tendon forces for the routing shown in Fig. 7. Detailed numerical values of the manipulating system used for the simulation are given in Lee (1991). Note that an amount of pretensioning torque has been added to each motor to ensure positive tension in every tendon. The differences in motor torques and tendon forces responses are due to the inertia and viscous effect of the rotors. It can be concluded that without proper biased forces, negative tension may occur in tendons.

7. Summary

A systematic methodology for the resolution of joint torque signals to motor torque signals in tendon-driven manipulators has been developed. This technique uses circuit-like equations to transform torques from the joint space and the tendon (or motor) space. Three different kinematic structures have been used to illustrate the methodology.

The technique has also been demonstrated by the simulation of a three-DOF manipulating system. The technique can be easily programmed on a digital computer or implemented into an analog-circuit system. It is hoped that this technique can make real-time control using computed torque method feasible.

Acknowledgement

This research has been supported in part by the Department of Energy, Grant No. DEFG05-88ER13977, and in part by the NSF's Engineering Research Centers Program, NSFD CDR 8803012. Such supports do not constitute an endorsement by the supporting agencies of the views expressed in the article.

References

Jacobsen, S. C., Wood, J. E., Knutti, D. F., and Biggers, K. B., 1984, "The Utah/MIT Dextrous Hand: Work in Progress," The Intl. Journal of Robotics Research, Vol. 3, No. 4, pp. 21-50.

Jacobsen, S. C., Ko, H., Iversen, E. K., and Davis, C. C., 1989, "Antagonistic Control of a Tendon Driven Manipulator," Proc. of IEEE Intl. Conference on Robotics and Automation, pp. 1334-1339.

Lee, J. J., 1991, "Tendon-Driven Manipulators: Analysis, Synthesis, and Control," Ph.D. Dissertation, Dept. of Mechanical Engineering, The University of Maryland, College Park, MD.

Lee, J. J., and Tsai, L. W., 1991, "On the Structural Synthesis of Tendon-Driven Manipulators Having Pseudo-Triangular Matrix", The Intl. Journal of Robotics Research, Vol. 10, No. 3.

Morecki, A., Busko, Z., Gasztold, H., and Jaworek, K., 1980, "Synthesis and Control of the Anthropomorphic Two-Handed Manipulator," Proc. of the 10^{th} Intl. Symposium on Industrial Robots, Milan, Italy, pp. 461-474.

Okada, T., 1977, "On a Versatile Finger System," Proc. of the 7^{th} Intl. Symposium on Industrial Robots, Tokyo, Japan, pp. 345-352.

Paul, R. P., 1981, *Robot Manipulator: Mathematics, Programming and Control*, MIT Press, Cambridge, MA.

Pham, D. T., and Heginbotham, W. B., 1986, *Robot Grippers,* IFS (Publications) Ltd., UK., Springer-Verlag.

Salisbury, J. K., 1982, "Kinematic and Force Analysis of Articulated Hands," Ph.D. Dissertation, Dept. of Mechanical Engineering, Stanford University, Stanford, CA.

Strang, G., 1980, *Linear Algebra and Its Applications*, Academic Press, Inc., Orlando, FL.

Tsai, L. W., and Lee, J. J., 1989, "Kinematic Analysis of Tendon-Driven Robotic Mechanisms Using Graph Theory," ASME J. of Mechanisms, Transmissions, and Automation in Design. Vol. 111, No.1, pp. 59-65.

Figure Captions

Fig. 1 An n-DOF tendon-driven manipulator with $n + 1$ tendons

Fig. 2 Schematic of the motor-tendon spooling system

Fig. 3 A one-DOF system

Fig. 4 Characteristics of $O^+(x)$ and $O^-(x)$

Fig. 5 Free-body diagrams of a three-DOF tendon-driven manipulator

Fig. 6 Kinematic structure of the Stanford/JPL Finger

Fig. 7 A fully coupled kinematic structure

Fig. 8 Control block diagram of a three-DOF tendon-driven manipulator

Fig. 9(a) Design details of the controller shown in Fig. 8

Fig. 9(b) Design details of the torque resolver shown in Fig. 8

Fig. 10 The schematic of a spatial three-DOF manipulator

Fig. 11 Motor torque response for the kinematic structure shown in Fig. 7, peak value = 7.64 $\times 10^4$ dyne-cm

Fig. 12 Tendon force response, B = 1.67 $\times 10^4$ dyne

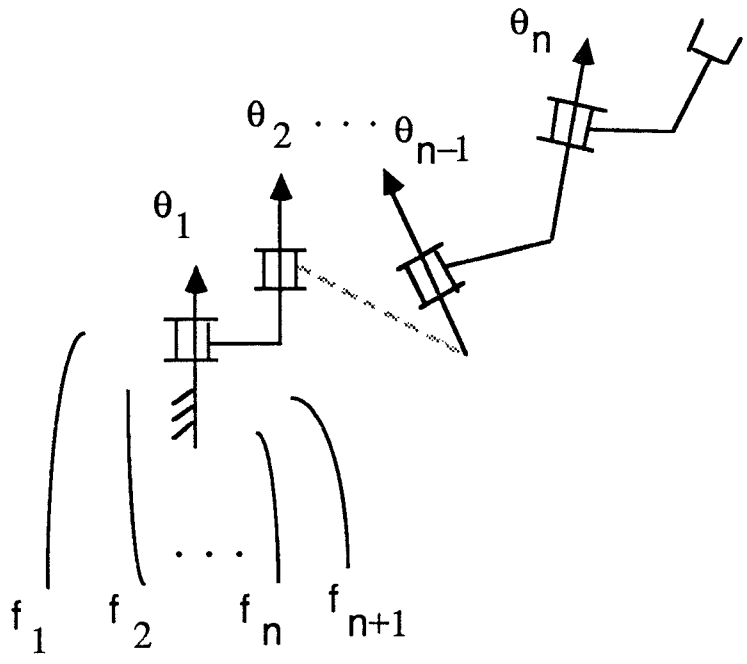

Fig. 1 An n-DOF tendon-driven manipulator
with n+1 tendons

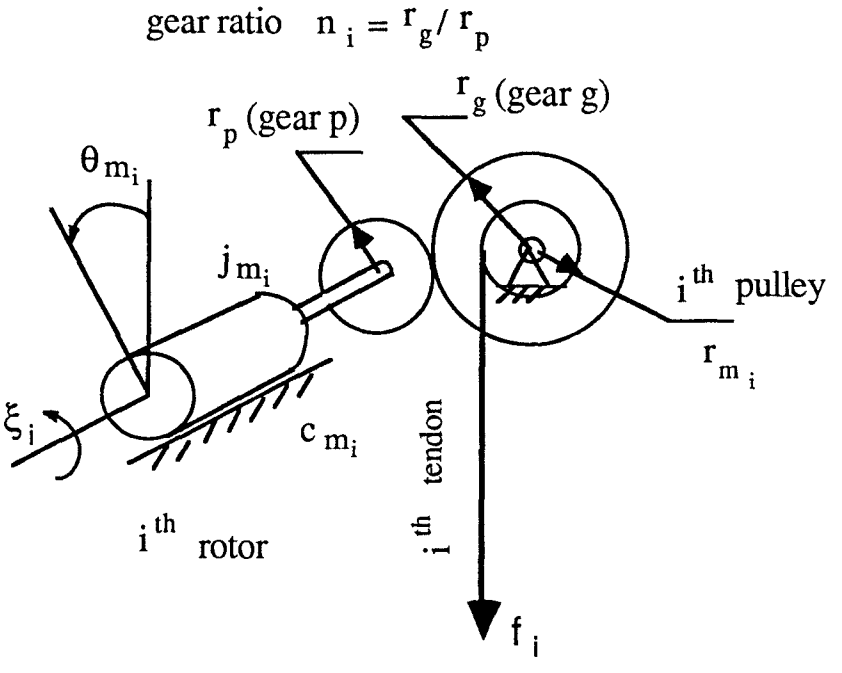

Fig. 2 Schematic of the motor-tendon spooling system

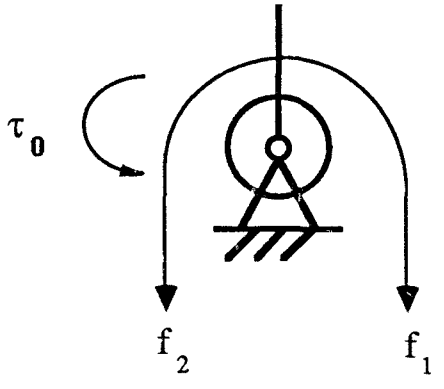

Fig. 3 A one-DOF tendon-driven manipulator

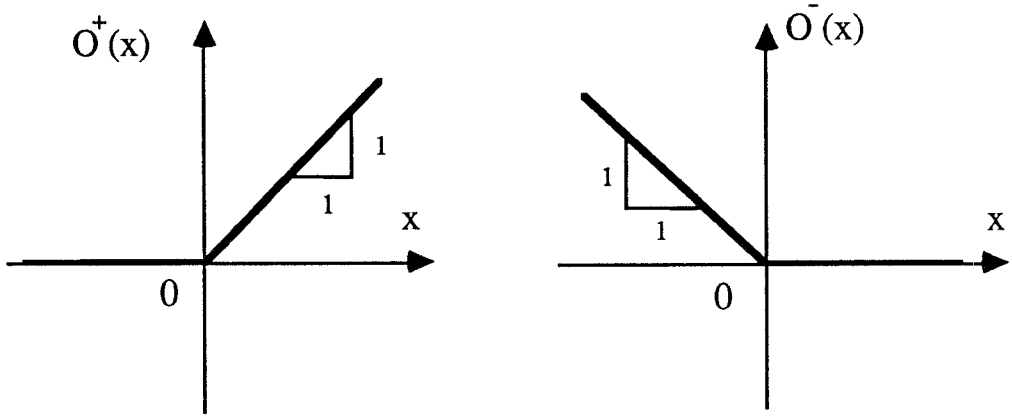

Fig. 4 Characteristics of $O^{+}(x)$ and $O^{-}(x)$

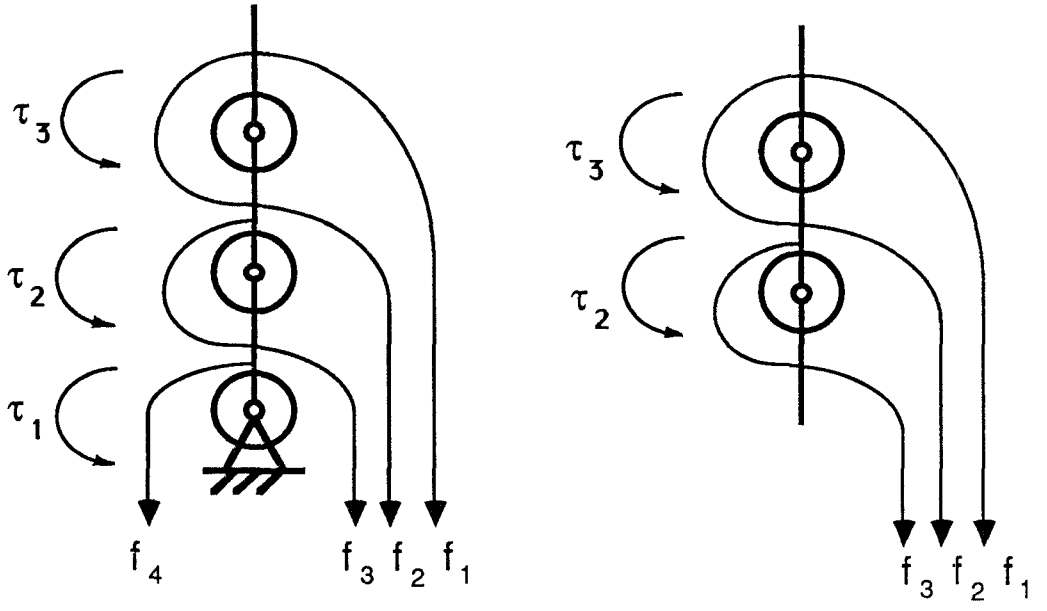

(a) (b)

Fig. 5 Free-body diagrams of a three-DOF tendon-driven manipulator

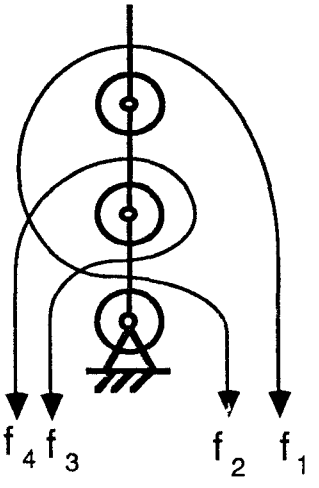

Fig. 6 Kinematic Structure of the Stanford/JPL Finger

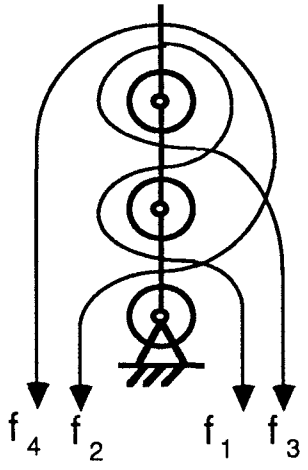

Fig. 7 A fully coupled kinematic structure

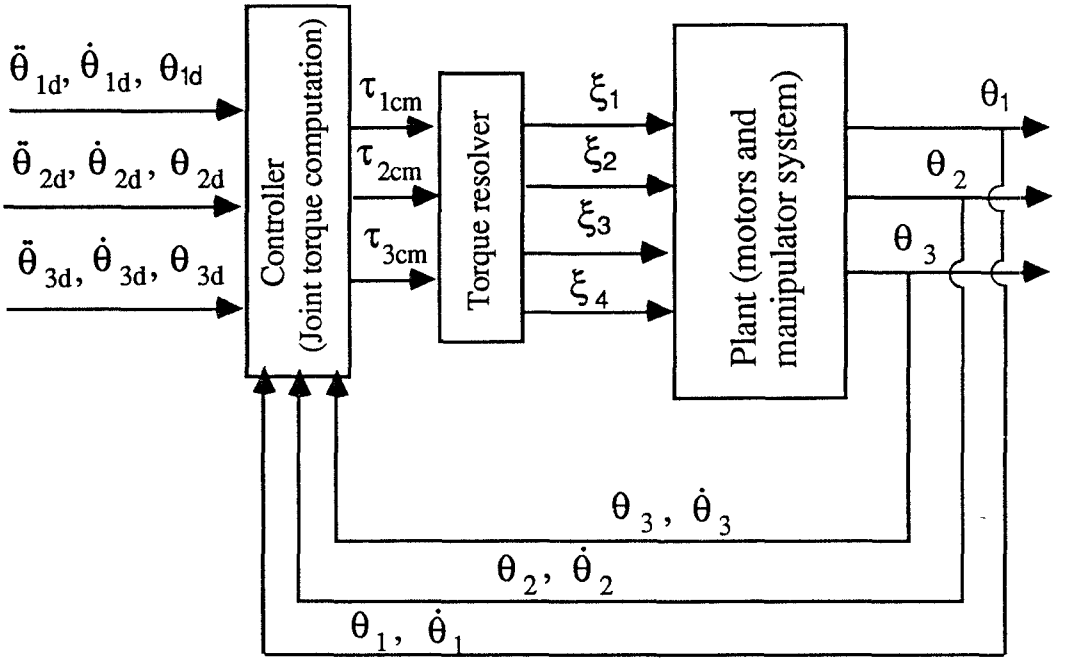

Fig. 8 Control block diagram of a three-DOF tendon-driven manipulator

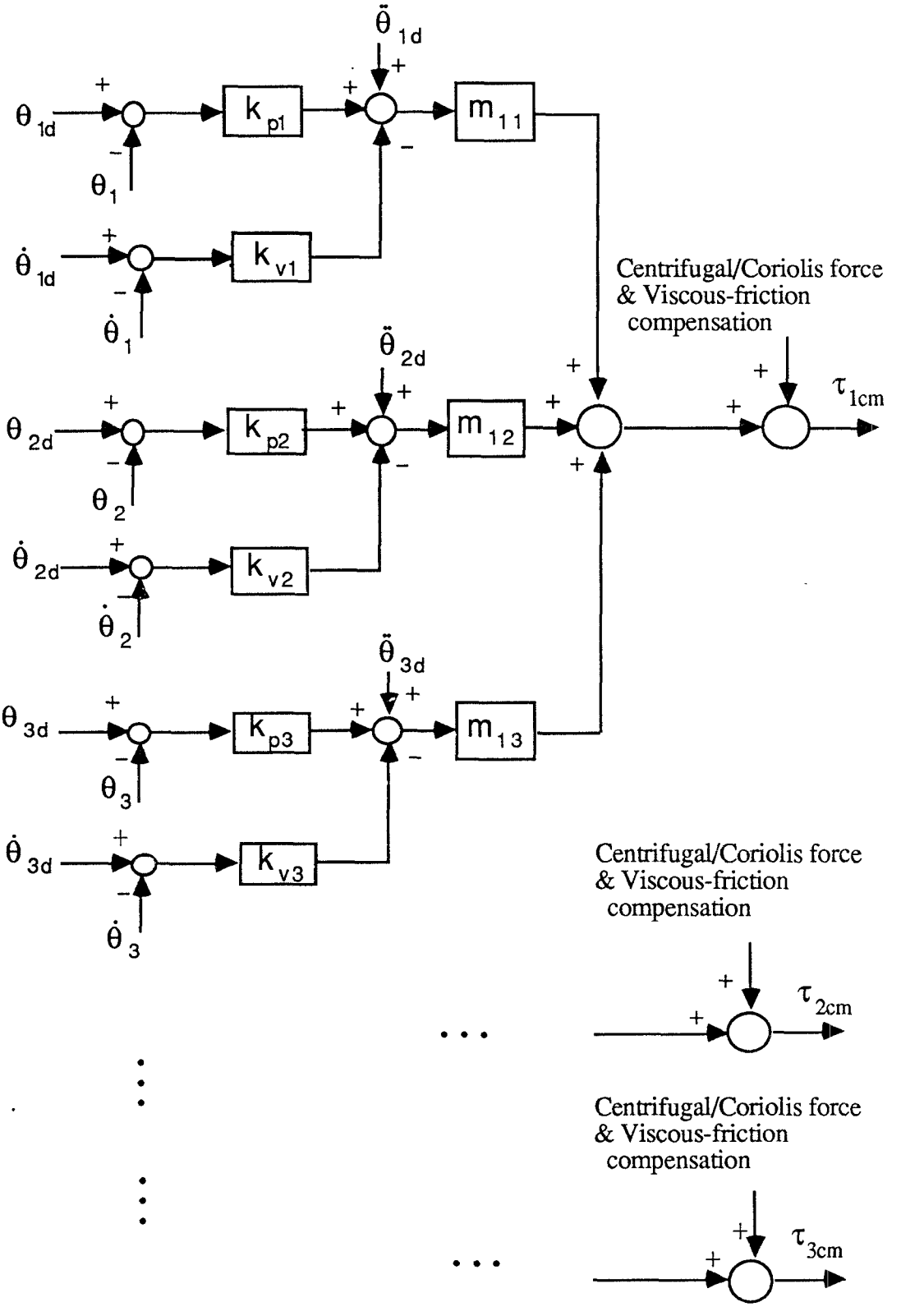

Fig. 9(a) Design details of the controller shown in Fig. 8

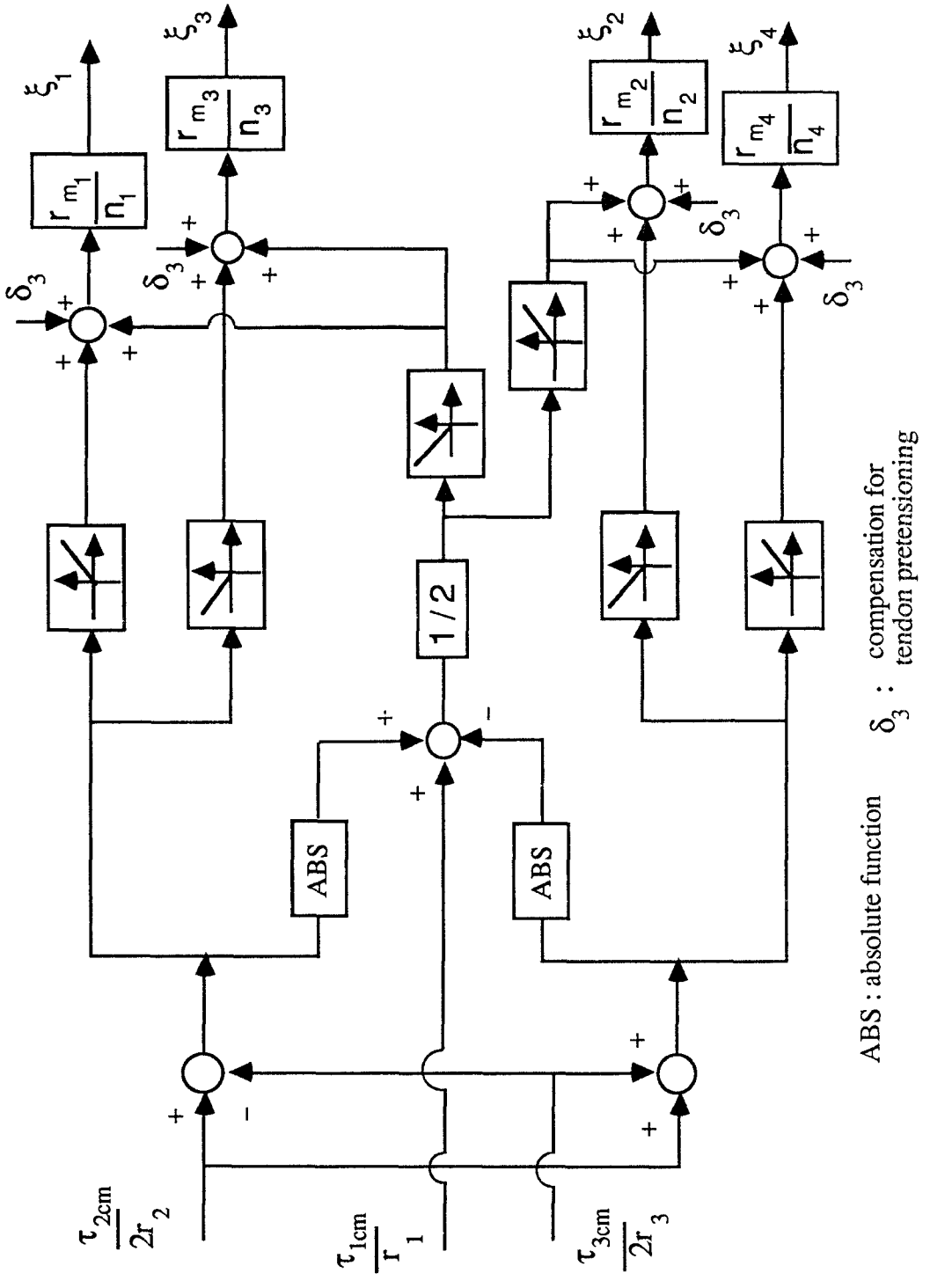

Fig. 9(b) Design details of the resolver shown in Fig. 8

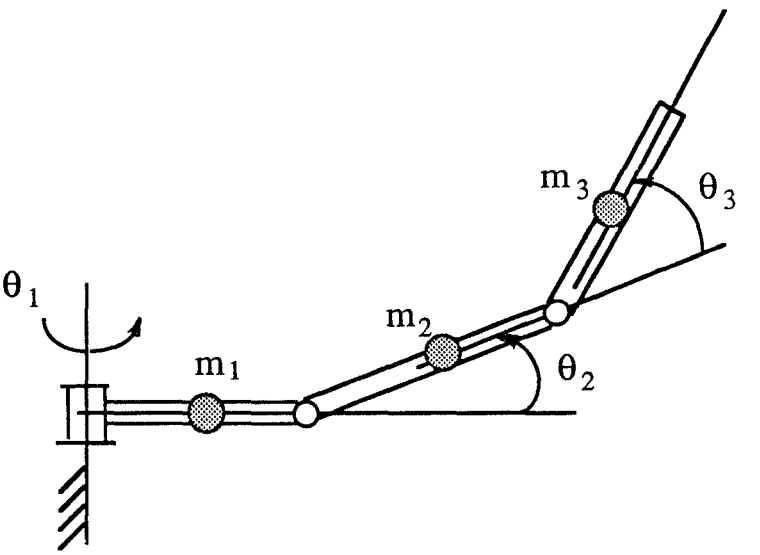

Fig. 10 Schematic of a spatial three-DOF manipulator

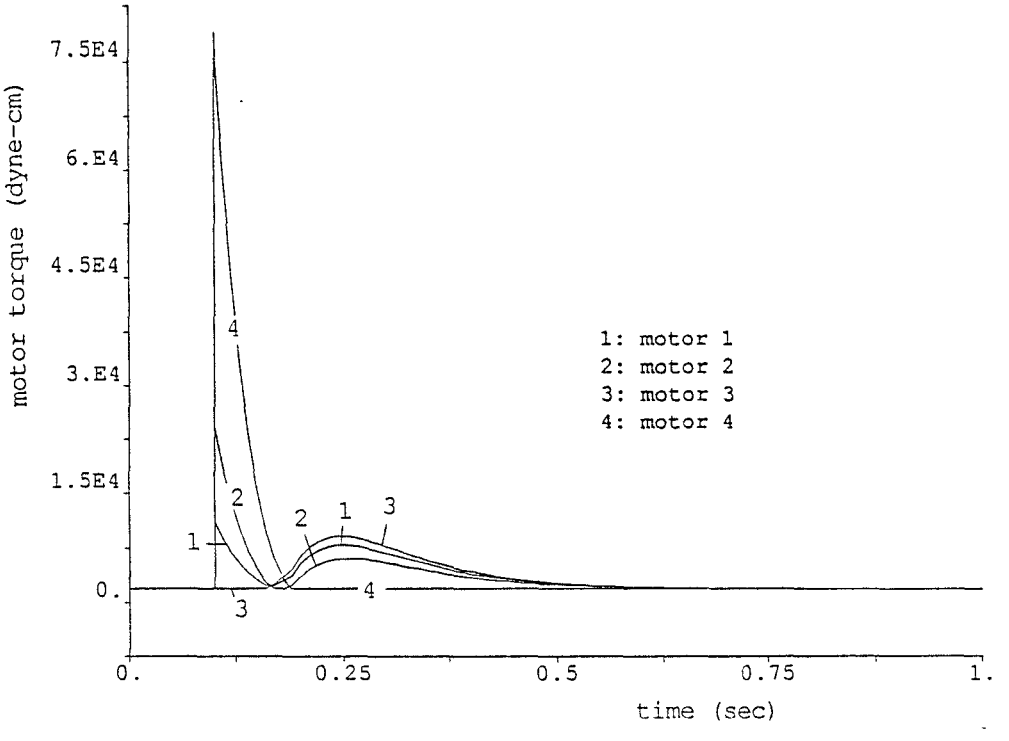

Fig. 11 Motor torque response for the kinematic structure shown in Fig. 7, peak value= 7.64 $\times 10^4$ dyne-cm

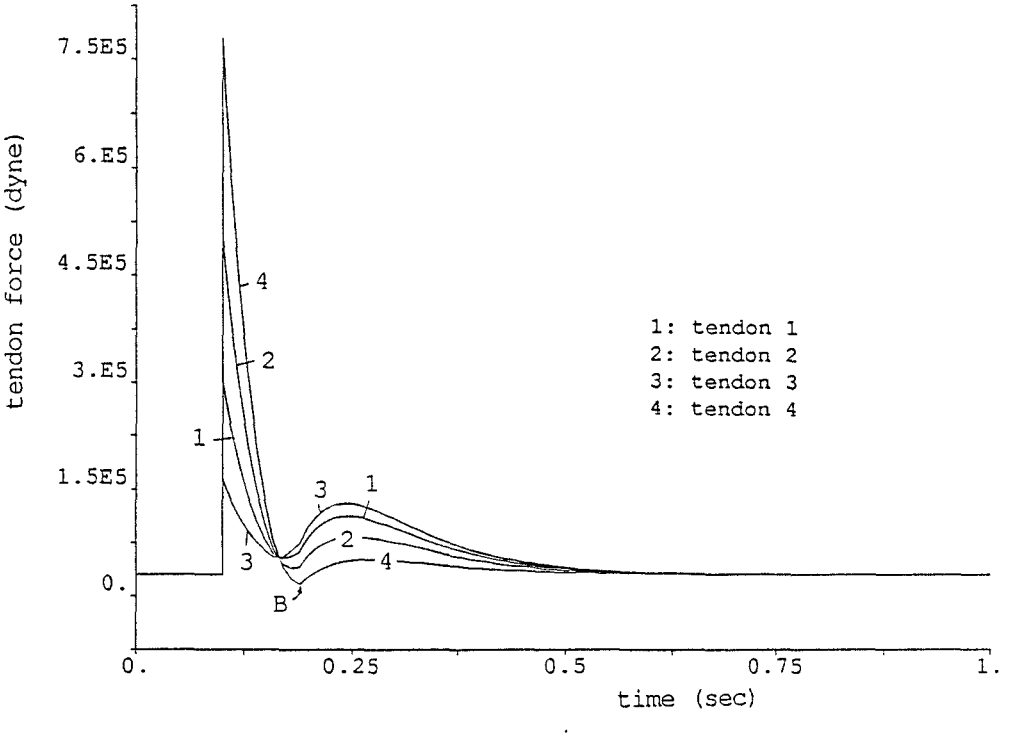

Fig. 12 Tendon force response, B= 1.67 $\times 10^4$ dyne